

DYNAMIC GROWTH OF AN EDGE CRACK IN A HALF SPACE

P. BURGERS† and L. B. FREUND‡
Division of Engineering, Brown University, Providence, RI 02912, U.S.A.

(Received 13 December 1978; received for publication 29 June 1979)

Abstract—The problem of an edge crack, propagating with constant velocity perpendicular to the boundary of a linear elastic half space, is solved numerically for typical self-similar loading cases. A limiting case of uniform pressure on the crack faces is shown to have a stress intensity factor close to that for the equivalent static problem, which serves as a check on the method. The effect of stress gradients is demonstrated and for impact loading, it is shown that cracks can only initiate under the center of the load if friction is present, and then only at very low crack tip speeds.

1. INTRODUCTION

Understanding of surface damage problems due to impact loads [1, 2] and dynamic indentation problems is hindered by the lack of solutions for crack problems in which a boundary, other than the crack surfaces, affects the dynamic stress distribution. So that resort need not be made to numerical schemes, such as finite elements or finite differences, a self-similar problem in dynamic linear elasticity is considered. This means there is no characteristic length in the problem and therefore the usual transform methods may be applied.

The problem considered is for an edge crack propagating perpendicular to the surface of an infinite half-space, having started with zero initial length at time $t = 0$, see Fig. 1(a). The loading systems considered have the property of retaining the self-similar nature of the problem. The solution method is similar to that used in static crack problems [3] in which the crack is represented by a continuous array of dislocations. For the dynamic problem, the fundamental solution is for a moving edge dislocation of constant Burgers vector, propagating with constant velocity from the boundary and perpendicular to it. The superposition parameter is the velocity of the dislocations, varying from zero to the velocity of the crack tip, V_{CT} .

In order to check the solution method, the limiting case of the static edge crack problem is used and compared with the result obtained by Koiter [4]. A number of loading cases which have practical interest are then considered.

2. FUNDAMENTAL SOLUTION

The fundamental solution used will be the dynamic stress distribution resulting from an edge dislocation, starting at time $t = 0$ at the surface of an infinite half-space and propagating with constant velocity, v , perpendicular to the boundary. A Cartesian coordinate system is introduced in the body such that $z = 0$ is the surface of the half-space, the z -axis is the line along which the dislocation propagates (and also the crack line) so that the z -coordinate specifies the position of the dislocation and the y -axis lies in the plane of the dislocation (and the crack), see Fig. 1(b). Letting σ_{xx} , σ_{xz} , σ_{zz} denote the relevant stress components and u_x , u_z denote the

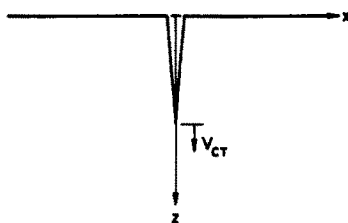


Fig. 1(a).

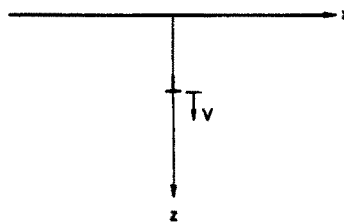


Fig. 1(b).

†Research Assistant, Division of Engineering, Brown University, Providence, RI 02912, U.S.A. (Effective 1 February, Post Doctoral Fellow, Department of Civil Engineering, Northwestern University, Evanston, IL 60201, U.S.A.)

‡Professor, Division of Engineering, Brown University, Providence, RI 02912, U.S.A.

non-zero displacement components, the traction free boundary condition on the surface of the half-space requires $\sigma_{zz} = \sigma_{zx} = 0$ on $z = 0$ and by symmetry $u_x = \sigma_{zx} = 0$ on $x = 0$. The last observation allows this problem to be solved by using the superposition of two simpler problems, the solutions of which are now given.

Problem 1. A Cartesian coordinate system is introduced in an infinite space so that the z - and x -axes line up with the previously described coordinate system. At time $t = 0$ two edge dislocations, with Burgers vectors of equal magnitude but opposite sign, appear at the origin of the infinite space and propagate along the z -axis in opposite directions with constant velocity v . From symmetry $u_x = \sigma_{zx} = 0$ on $x = 0$, satisfying the symmetry conditions of the fundamental solution and $u_z = \sigma_{zz} = 0$ on $z = 0$.

To obtain the fundamental solution, a layer of body force is applied along $z = 0$ to cancel out the resulting σ_{zz} stresses on $z = 0$. The solution obtained will satisfy the boundary and symmetry conditions of the fundamental solution and therefore by uniqueness in linear elastodynamics, must be the correct solution.

In view of the anti-symmetry with respect to the plane $x = 0$, consideration is limited to the solution of the problem in the half-space $-\infty < z < \infty$, $x \geq 0$. The boundary conditions on $x = 0$ are

$$u_x = \begin{cases} \Delta H(vt - z), & z > 0, \\ \Delta H(vt + z), & z < 0, \end{cases} \quad (2.1)$$

$$\sigma_{zx} = 0, \quad -\infty < z < \infty, \quad (2.2)$$

$$\sigma_{zz} = 0, \quad -\infty < z < \infty, \quad (2.3)$$

where Δ is the magnitude of the Burgers vector and H represents the unit step function. The problem is completely specified by imposing zero initial data and requiring the solution to satisfy the partial differential equations governing the motion of a linear elastic solid.

The displacement potentials for longitudinal and shear waves, ϕ and ψ , are introduced and these functions satisfy the usual wave equations. For the longitudinal wave potential ϕ , the equation is

$$\frac{\partial^2 \phi}{\partial x^2} + \frac{\partial^2 \phi}{\partial z^2} - a^2 \frac{\partial^2 \phi}{\partial t^2} = 0, \quad (2.4)$$

where a^{-1} is the longitudinal wave speed of the material. The shear wave potential ψ is governed by the same equation with " a " replaced by " b ", where b^{-1} is the shear wave speed.

The solution of the problem is now obtained by making use of integral transform methods. The time t is first eliminated by application of the one-sided Laplace transform[5]

$$\hat{f}(x, z, s) = \int_0^\infty f(x, z, t) e^{-st} dt, \quad (2.5)$$

where s may be viewed as a positive real number. Next the z dependence is suppressed by taking the two-sided Laplace transform

$$F(x, \lambda, s) = \int_{-\infty}^\infty \hat{f}(x, z, s) e^{-\lambda z} dz. \quad (2.6)$$

The convention established in (2.5) and (2.6) by which the symbol $\hat{}$ is used to denote the transform on t and an upper case letter to denote the transform on z is followed in the subsequent analysis.

Application of the transforms to the equations governing ϕ and ψ yields two ordinary differential equations whose solutions, bounded as $x \rightarrow \infty$, are

$$\Phi(x, \lambda, s) = s^{-3} P(\lambda) e^{-\alpha x}, \quad \text{Re}(\alpha) \geq 0, \quad (2.7)$$

$$\Psi(x, \lambda, s) = s^{-3} Q(\lambda) e^{-\beta x}, \quad \text{Re}(\beta) \geq 0, \quad (2.8)$$

where

$$\alpha = (a^2 - \lambda^2)^{1/2}, \quad \beta = (b^2 - \lambda^2)^{1/2}, \quad (2.9)$$

and appropriate cuts are introduced to ensure $\text{Re}(\alpha, \beta) \geq 0$ everywhere in the λ -plane. The functions P, Q are unknown and their coefficients are chosen so that they are independent of s . Application of the transforms to the boundary conditions (2.1)–(2.3) yields

$$U(0, \lambda, s) = -\frac{\alpha}{s^2}P - \frac{\lambda}{s^2}Q = \frac{2d\Delta}{s^2(d^2 - \lambda^2)},$$

and

$$\Sigma_{xz}(0, \lambda, s) = -\frac{2\alpha\lambda}{s}P + \frac{(b^2 - \lambda^2)}{s}Q = 0,$$

where $d = 1/v$ is the slowness of the dislocation.

The transformed stresses of interest are

$$\Sigma_{zz}(x, \lambda, s) = -\frac{2d\Delta\mu}{sb^2} \left\{ \frac{b^2 - 2\lambda^2}{\alpha(d^2 - \lambda^2)} (b^2 - 2a^2 + 2\lambda^2) e^{-sax} - \frac{4\lambda^2\beta}{d^2 - \lambda^2} e^{-s\beta x} \right\}, \quad (2.10)$$

$$\Sigma_{xx}(0, \lambda, s) = -\frac{2d\Delta\mu}{sb^2} \frac{R(\lambda)}{(d^2 - \lambda^2)\alpha}, \quad (2.11)$$

where μ is the shear modulus, $R(\lambda)$ is the Rayleigh wave function defined by

$$R(\lambda) = (b^2 - 2\lambda^2)^2 + 4\alpha\beta\lambda^2, \quad (2.12)$$

and α, β are given in eqn (2.9).

The inversion of eqns (2.10) and (2.11) is ideally suited to the Cagniard de Hoop method[5]. The σ_{zz} stress on $z = 0$ found in this manner is

$$\sigma_{zz}(x, 0, t; d) = -\frac{\Delta}{x} \frac{2d\mu}{\pi b^2} \left\{ \frac{(b^2 - 2a^2 + 2\omega^2)}{(d^2 - a^2 + \omega^2)} \frac{(b^2 - 2\omega^2)}{\sqrt{(\omega^2 - a^2)}} H(\omega - a) + 4 \frac{(\omega^2 - b^2)^{1/2}}{(d^2 - b^2 + \omega^2)} \omega^2 H(\omega - b) \right\}_{\omega=it/x}. \quad (2.13)$$

The σ_{xx} stress on $x = 0$ can be treated in a similar manner as eqn (2.23) in [6] to give

$$\sigma_{xx}(0, z, t; d) = -\frac{\Delta}{z} \frac{2v\mu}{\pi b^2} \left\{ \text{Im} \left[\frac{R(-\omega)}{\alpha(-\omega)} \right] \cdot \frac{1}{\omega^2} \frac{1}{(1/d - 1/\omega)} \frac{H(\omega - a)}{(1/d + 1/\omega)} \right\}_{\omega=it/z}. \quad (2.14)$$

The singularity in σ_{xx} when $1/\omega$ approaches $1/d$ will allow the original problem to be formulated as a Cauchy singular integral equation.

Problem 2. The $\sigma_{zz}(x, 0, t)$ stress distribution derived in Problem 1 gives the negative of the required body force distribution needed to satisfy the $\sigma_{zz}(x, 0, t) = 0$ boundary condition in the fundamental solution. The following argument to obtain Problem 2 follows that given by Freund[7] with only slight modification. Examining eqn (2.13), it is observed that $\sigma_{zz}(x, 0, t)$ is a function of the form $f(\omega)/x$. This implies that a stress level of magnitude $1/x$ radiates out along the x -axis at a constant speed. In particular, a stress level of $f(\omega)/x$ radiates out with speed $u = 1/\omega$ where the speed u varies between zero and the longitudinal wave speed. The x -coordinates at time t of stress levels moving with speeds u and $u + du$ are ut and $(u + du)t$,

respectively. Therefore, to within first-order terms in the infinitesimal quantity du , the resultant force due to all stress levels with speeds between u and $u + du$ is $t/xf(1/u) du$ acting at $x = ut$.

Let a Cartesian coordinate system defined on a half-space as for the fundamental solution. The solution to Problem 2 is then the dynamic stress distribution resulting from the following problem. At time $t = 0$, two concentrated forces of magnitude $1/u$, pointing in the negative z direction, appear at the origin and immediately propagate out with speed u , one in the $-x$ direction and the other in the $+x$ direction. The boundary conditions for this problem are

$$\sigma_{zz}(x, 0, t) = \begin{cases} \Delta t/x\delta(ut - x), & x > 0, \\ -\Delta t/x\delta(ut + x), & x < 0, \end{cases} \quad (2.15)$$

$$\sigma_{zz}(x, 0, t) = 0, \quad -\infty < x < \infty, \quad (2.16)$$

where δ is the Dirac delta function. Imposing zero initial conditions and requiring the solution satisfy the governing equations of motion for a linear elastic solids, completes the specification of the problem. Solving Problem 2 in a similar manner to Problem 1, gives

$$\begin{aligned} \sigma_{zz}(0, z, t; \omega) = & \frac{2\Delta\omega^3}{\pi z} \left\{ \frac{(b^2 - 2a^2 + 2\omega^2)(b^2 - 2\omega^2)\omega H(\omega - a)}{(\omega^2 - a^2 + \omega^2)\mathcal{R}(i\sqrt{\omega^2 - a^2})\sqrt{(\omega^2 - a^2)^{1/2}}} \right. \\ & \left. + \frac{4(\omega^2 - b^2)^{1/2}(a^2 - b^2 + \omega^2)^{1/2}\omega^2}{(\omega^2 + b^2 + \omega^2)\mathcal{R}(i\sqrt{\omega^2 - b^2})} H(\omega - b) \right\}_{\omega = t/z} \end{aligned} \quad (2.17)$$

where $\omega = 1/u$.

The fundamental solution may now be written down, using the solutions of Problems 1 and a superposition of Problem 2. The result is

$$\begin{aligned} \sigma_{zz}(0, z, t; d) = & \frac{\Delta}{z} \frac{2d}{\pi b^2} \mu \left\{ \text{Im} \left[\frac{\mathcal{R}(-\lambda)}{(d^2 - \lambda^2)\alpha(-\lambda)} \right] H(\lambda - a) \right. \\ & + \int_0^{1/a} \left[\frac{(b^2 - 2a^2 + 2\omega^2)(b^2 - 2\omega^2)}{(d^2 - a^2 + \omega^2)\sqrt{(\omega^2 - a^2)^{1/2}}} H(\omega - a) + \frac{4(\omega^2 - b^2)^{1/2}\omega^2 H(\omega - b)}{(d^2 - b^2 + \omega^2)} \right] \\ & \times \frac{2\omega^3}{\pi} \left[\frac{(b^2 - 2a^2 + 2\lambda^2)(b^2 - 2\lambda^2)}{(\omega^2 - a^2 + \lambda^2)\mathcal{R}(i\sqrt{\lambda^2 - a^2})} \frac{\lambda}{\sqrt{(\lambda^2 - a^2)^{1/2}}} H(\lambda - a) \right. \\ & \left. \left. + \frac{4(\lambda^2 - b^2)^{1/2}(a^2 - b^2 + \lambda^2)^{1/2}}{(\omega^2 - b^2 + \lambda^2)\mathcal{R}(i\sqrt{\lambda^2 - b^2})} \lambda^2 H(\lambda - b) \right] d(1/\omega) \right\}_{\lambda = t/z}, \end{aligned} \quad (2.18)$$

where Δ is the Burgers vector of the edge dislocation in the half-space.

The integrand in eqn (18) must be evaluated numerically and to do this a number of features should be noted. Firstly, as $(1/\omega) \rightarrow 0$, the integrand goes to a finite limit and, secondly, as $\omega \rightarrow a, b$ the integrand is $O(1/(\omega - a)^{1/2})$, $O((\omega^2 - b^2)^{1/2})$, respectively. The integral was evaluated using Simpson's Rule [8] with 101 integration points. A typical result for the $\sigma_{zz}(0, z, t; d)$ stress for $1/d = 1/(2b)$ is given in Fig. 2.

For convenience, let σ_{zz}^{FS} represent the previous result when Δ has magnitude one.

3. SINGULAR INTEGRAL EQUATION

Having constructed a fundamental solution, the object is to solve the problem of an edge crack suddenly appearing at the surface of a half-space and propagating with velocity V_{CT} (less than the Rayleigh wave speed), perpendicular to the boundary of the half-space (along the z -axis). To do this, a solution is built up using the previous result by introducing a continuous array of moving dislocations, each moving with velocity $v \ll V_{CT}$ with a density function [9], $\mu(v)$, so that $\mu(v)dv$ represents the infinitesimal Burgers vector of an edge dislocation propagating with velocity v .

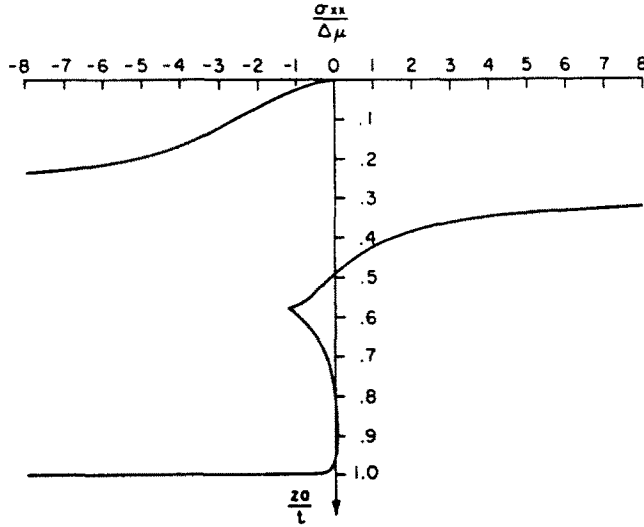


Fig. 2. $\sigma_{xx}(0, z, t)$ due to edge dislocation in Fig. 1(b).

The resulting stress distribution along the crack line is given by

$$\sigma_{xx}(0, z, t) = \sigma_{xx}^{Loads}(0, z, t) + \int_0^{V_{CT}} \sigma_{xx}^{FS}\left(0, z, t; \frac{1}{v}\right) \mu(v) dv, \tag{3.1}$$

where σ_{xx}^{Loads} is the stress due to the applied loads on the half space (without an edge crack) and $\mu(v)$ is unspecified for the present, apart from satisfying certain smoothness requirements. The integral must be interpreted in the Cauchy principal value sense because, when $z/t \leq V_{CT}$, there is a pole at $z/t = v$.

The singular integral equation is obtained by requiring the stresses on the crack face to satisfy the correct boundary conditions. Considering the case when the crack face is traction free, the resulting singular integral equation is given by

$$-\sigma_{xx}^{Loads}(0, z, t) = \int_0^{V_{CT}} \sigma_{xx}^{FS}\left(0, z, t; \frac{1}{v}\right) \mu(v) dv, \quad v \leq V_{CT}, \quad 0 \leq z \leq V_{CT}t \tag{3.2}$$

where the left-hand side is a known function and $\mu(v)$ has to be determined. This is the standard form of an integral equation with a Cauchy-type kernel and the numerical solution of such equations has received much attention recently by a number of authors, e.g. Erdogan *et al.*[10, 11]. The numerical solution of eqn (1) is based on a method developed by Erdogan *et al.*[11] with some modifications used by Lo[12] in analyzing branched cracks.

From an asymptotic solution about the crack tip [10], it is known that quantities like stresses, strains and the dislocation density function are $O(1/(V_{CT} - v)^{1/2})$ as $(V_{CT} - v) \rightarrow 0^+$. The behavior at $v = 0$ is more difficult to obtain but providing the loading cases considered have σ_{xx} stresses that are $O(1/z^{1/2})$ as $z \rightarrow 0^+$ then the behavior of $\mu(v)$ as $v \rightarrow 0^+$ must be less singular than that for a closed crack. That is $\mu(v) = O(1/v^{1/2})$ as v tends to 0^+ .

A new function $F(v)$ is introduced such that

$$\mu(v) = \frac{F(v)}{(V_{CT} - v)^{1/2} v^{1/2}} \tag{3.3}$$

where $F(v)$ is finite at $v = V_{CT}$ and is zero at $v = 0$. Substituting for $\mu(v)$ in (2) results in

$$\frac{1}{z} \int_0^{V_{CT}} \frac{f(v, z/t)}{v - z/t} \frac{F(v) dv}{(V_{CT} - v)^{1/2} v^{1/2}} + \frac{1}{z} \int_0^{V_{CT}} k(v, z/t) \frac{F(v)}{(V_{CT} - v)^{1/2} v^{1/2}} dv = g(z, t), \quad 0 \leq z/t \leq V_{CT}, \tag{3.4}$$

where

$$\sigma_{xx}^{FS}\left(0, z, t; \frac{1}{v}\right) = \frac{f(v, z/t)}{z(v - z/t)} + \frac{k(v, z/t)}{z}.$$

This equation is ideally suited for numerical solution by the method presented in [10], a brief outline of which is given in Appendix A.

4. STRESS INTENSITY FACTOR CALCULATION

Of primary importance in the analysis of a linear elastic solid containing a crack is the stress intensity factor K , defined for Mode I problems (which are the only cases considered here) by

$$K_I = \lim_{(z - V_{CT}t) \rightarrow 0^+} \sqrt{(2\pi)(z - V_{CT}t)^{1/2}} \sigma_{xx}(0, z, t). \quad (4.1)$$

From the resulting stress distribution on the crack line given by (3.1) after substitution of (2.18), it is obvious that the only part of σ_{xx}^{FS} that will contribute to the stress intensity factor is the stress due to a dislocation in the full space.

After rewriting (3.1) in terms of

$$u = (V_{CT} - v)/(zt - V_{CT})$$

and taking the appropriate limit, the stress intensity factor is obtained as

$$K = -\sqrt{(2\pi)} \frac{\mu}{b^2} \frac{V_{CT}}{(V_{CT}t)^{1/2}} F(V_{CT}) \frac{\text{Re}[R(-1/V_{CT})]}{(1/V_{CT}^2 - a^2)^{1/2}}. \quad (4.2)$$

For problems in which $\sigma_{xx}^{\text{Loads}}(0, z, t)$ can be written as $g(z/t)/z$, the integral equation need only be solved once for any crack tip velocity since (3.1) can be written in terms of (z/t) only. The loading systems which do not have this feature require separate evaluations for each value of t .

5. LOADING CASES

All the loading cases suitable for use in this scheme must have the property of being self-similar. For all cases the initial conditions are taken to be zero at time $t = 0$.

Case 1. The boundary condition is uniform pressure on the crack faces, i.e.

$$\sigma_{xx}(0, z, t) = \Delta\mu, \quad 0 < z < V_{CT}t, \quad (5.1)$$

$$\sigma_{xx}(x, 0, t) = \sigma_{zz}(x, 0, t) = 0, \quad -\infty < x < \infty. \quad (5.2)$$

This example was used as a check on the solution method, see Appendix B.

Case 2. To obtain an example of a stress gradient along the crack faces, the following boundary conditions were used.

$$\sigma_{xx}(0, z, t) = \Delta\mu \frac{z}{V_{CT}t}, \quad 0 < z < V_{CT}t, \quad (5.3)$$

$$\sigma_{xx}(x, 0, t) = \sigma_{zz}(x, 0, t) = 0, \quad -\infty < x < \infty. \quad (5.4)$$

Case 3. Of great interest is the σ_{xx} stress distribution due to an elastic ball hitting a half space. Using the suggestion given in [2], that the initial response be approximated by a uniform pressure spreading out across the half space surface, the following boundary conditions were used.

$$\sigma_{xx}(0, z, t) = \begin{cases} \Delta\mu H(ut - x), & x > 0, \\ \Delta\mu H(ut + x), & x < 0, \end{cases} \quad (5.5)$$

$$\sigma_{xx}(0, z, t) = 0, \quad -\infty < x < \infty. \quad (5.6)$$

The best approximation is apparently obtained by the uniform pressure spreading out at a rate proportional to \sqrt{t} , but with the above method this is not possible to model. The σ_{xx} stress on the z-axis is

$$\sigma_{xx}(0, z, t) = \frac{2\mu}{\pi u} \int_0^{u/z} \left[\frac{(b^2 - 2a^2 + 2w^2)(b^2 - 2w^2)wH(w - a)}{(d^2 - a^2 + w^2)R(i\sqrt{[w^2 - a^2]})\sqrt{(w^2 - a^2)^{1/2}}} + \frac{4(w^2 - b^2)^{1/2}(a^2 - b^2 + w^2)^{1/2}}{(d^2 - b^2 + w^2)R(i\sqrt{[w^2 - b^2]})} w^2 H(w - b) \right]_{w=\pi/z} d\tau, \quad (5.7)$$

see Fig. 3.

Case 4. Of some importance is the effect of friction between the impacting body and the half space. This is modeled by a shear stress spreading out over the half space boundary, so that the boundary conditions are

$$\sigma_{xx}(0, z, t) = \begin{cases} -\Delta\mu H(ut - x), & x > 0, \\ \Delta\mu H(ut + x), & x < 0, \end{cases}$$

$$\sigma_{xz}(0, z, t) = 0, \quad -\infty < x < \infty,$$

and the resulting σ_{xx} stress is

$$\sigma_{xx}(0, z, t) = \frac{4\mu}{\pi} \int_0^{u/z} \left[\frac{(w^2 - a^2)^{1/2}(b^2 - a^2 + w^2)^{1/2}(b^2 - 2w^2)wH(w - a)}{(d^2 - a^2 + w^2)R(i\sqrt{[w^2 - a^2]})} - \frac{\sqrt{(w^2 - b^2)^{1/2}(b^2 - 2w^2)w^2 H(w - b)}}{(d^2 - b^2 + w^2)R(i\sqrt{[w^2 - b^2]})^{1/2}} \right]_{w=\pi/z} d\tau,$$

see Fig. 4.

Features that should be noted about that the σ_{xx} stresses on the z axis are that for Cases 3 and 4 there is a tensile region immediately behind the longitudinal wave front followed by a compressive zone, in which the stresses are bounded. In the region nearest to the surface the stresses are tensile.

6. RESULTS

For the loading cases considered, time may be used as a parameter with the result that the integral equation need only be solved for one time and the solutions at other times can be scaled accordingly. The stress intensity factor for these cases is then proportional to $(t/V_{CT})^{1/2}$. To obtain the solutions a value of $a^2/b^2 = 1/3$ was used, which corresponds to a Rayleigh wave speed of $0.919/b$. From [6] it can be concluded that for cracks with loadings less than square

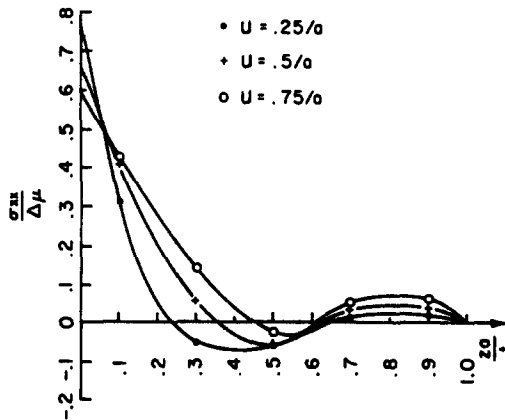


Fig. 3. $\sigma_{xx}(0, z, t)$ due to loading Case 3.

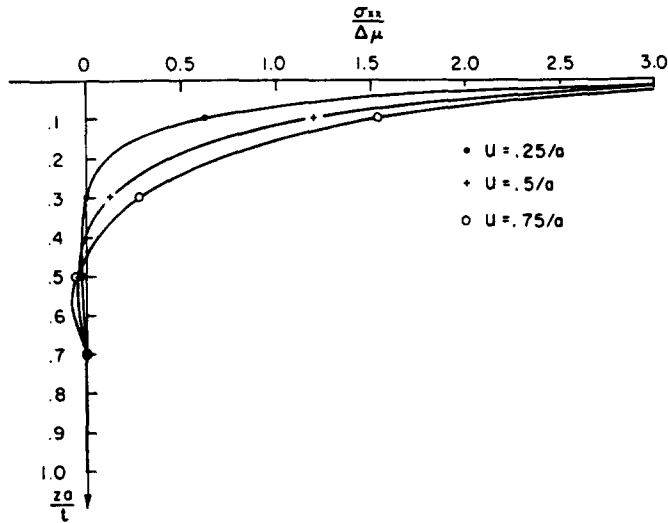


Fig. 4. $\sigma_{xx}(0, z, t)$ due to loading Case 4.

root singular at the crack tip and propagating with the Rayleigh wave speed, the energy release rate and therefore the stress intensity factor are zero. This allows one point on the graphs of K vs $V_{CT}b$ to be obtained.

The case of uniform pressure on the crack faces is used to obtain a check on the method. See Appendix B and Fig. 5. This is an example of problems not necessarily involving the impact of one body on another, e.g. the growth of an edge crack in a tensile sheet is of importance in shell structures. The ratio, G/G^* , where G is the energy release rate [9] and $G^* = \pi(\Delta\mu)^2(V_{CT}t)$ is plotted in Fig. 5 for Case 1. Noting that for the static case $G = (1.12)^2G^*$, where in G^* , instead of $(V_{CT}t)$, crack length is used, it can be seen that the range of V_{CT} for which G in the dynamic case is within 10% of the static value is fairly large, i.e. between 0 and $0.5/b$ approximately. This implies that the dynamic stress intensity will be within 5% of the static value for this range of crack tip velocities and gives some indication that the quasi-static result may be sufficiently accurate at low crack tip velocities for practical problems. Case 2 is considered as it gives some insight into the effect of stress gradients on the stress intensity factor, see Fig. 5. In comparing the K value for uniform pressure, $\Delta\mu$, and pressure varying as

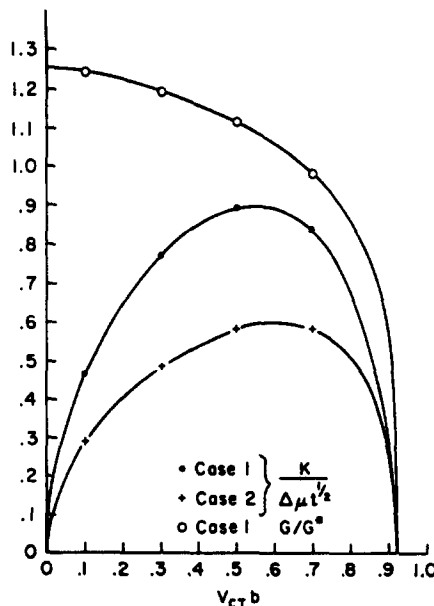


Fig. 5. Stress intensity factor vs crack tip velocity for loading Cases 1 and 2 and energy release rate vs crack tip velocity for loading Case 1.

$\Delta\mu z/(V_{CT}t)$, it is seen that although the total force exerted on the crack face in the latter case is only half that exerted in the former, the stress intensity factor is approximately 2/3 the K value for uniform pressure. This indicates that the stress gradient has a substantial effect which could have application in geological situations, e.g. pressurizing a fault with fluid escaping away from the fault line.

Cases 3 and 4 are of direct interest in impact problems, see Fig. 6. In both cases the rapid rise of K to a maximum value (for any fixed time) at a relatively low value of crack velocity, compared to the shear wave speed, is important. Assuming the approximation of an impact on an elastic half space as a uniform pressure distribution is reasonable, the effect of friction can be seen to play an important role. For an impact problem, the K value due to the applied σ_{zz} stress will be negative and with no other applied stresses there will be no tendency for an edge crack to propagate. However, if there is some friction between the impacting body and the half space, a stress distribution as in case 4 results. Assuming the coefficient of friction ν to be 0.3, and considering the case when $u = 0.25/a$, it can be seen from Fig. 6 that the positive K values due to the friction stresses will be larger than the negative K values due to the normal stresses for small values of crack velocity, i.e. for V_{CT} less than approximately $0.1/b$, which is in the range of observed crack propagation. For smaller values of ν , there will still be a region (with small V_{CT}) where the resulting value of K is positive. If higher values of speed u are used (modeling impact by a body with a higher velocity) the range of crack velocities for which K will be positive is larger. Obviously, the approximation of uniform pressure is only valid at best for short times and at longer times the pressure must decay. The above results do show, however, that initially, if crack propagation does occur, it will do so at relatively low velocities.

7. CONCLUSIONS

A series of superpositions is used to obtain the solution of an edge dislocation running perpendicular to the surface of a linear elastic half space. This is used as the fundamental solution in setting up a singular integral equation, to solve a self similar edge crack problem. By using a Gaussian integration scheme, specific examples can be solved by reducing the problem to a system of linear algebraic equations.

The effect of stress gradients on the crack faces is shown by comparing Cases 1 and 2 and the importance of frictional effects in impact problems is clearly demonstrated by Cases 3 and 4.

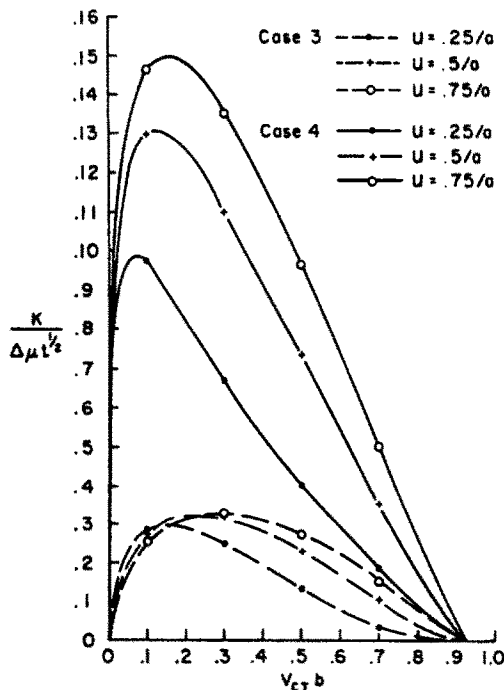


Fig. 6. Stress intensity factor vs crack tip velocity for loading Cases 3 and 4.

Acknowledgements—The authors are grateful for the support from the National Science Foundation through the Materials Research Laboratory at Brown University, and for helpful discussions with Professor D. A. Simons and Dr. F. Nilsson.

REFERENCES

1. A. G. Evans and T. R. Wilshaw, Dynamic solid particle damage in brittle materials.—an appraisal. *J. Mater. Sci.* **12**, 97–116 (1977).
2. A. G. Evans, On impact damage in the elastic response regime. In preparation.
3. J. R. Rice, Mathematical analysis in the mechanics of fracture. *Fracture*, (Edited by H. Liebowitz), Vol. 2, pp. 191–311. Academic Press, New York (1968).
4. W. T. Koiter, Discussion of Rectangular tensile sheet with symmetric edge cracks, by O. L. Bowie. *J. Appl. Mech.* **32**, 237 (1965).
5. J. D. Achenbach, *Wave Propagation in Elastic Solids*. North-Holland, Amsterdam (1975).
6. L. B. Freund, Crack propagation in an elastic solid subjected to general loading—I. Constant rate of extension. *J. Mech. Phys. Solids* **20**, 129–140 (1972).
7. L. B. Freund, Crack propagation in an elastic solid subjected to general loading—II. Nonuniform rate of extension. *J. Mech. Phys. Solids* **20**, 141–152 (1972).
8. *Handbook of Mathematical Functions* (Edited by M. Abramowitz and I. A. Stegun). Dover, New York (1970).
9. L. B. Freund, The analysis of elastodynamic crack tip stress fields. *Mechanics Today*, (Edited by S. Nemat-Nasser), Vol. 3. Pergamon Press, Oxford (1976).
10. F. Erdogan and G. D. Gupta, On the numerical solution of singular integral equations. *Quarterly Appl. Math.* **30**, 525–534 (1972).
11. F. Erdogan, G. D. Gupta and T. S. Cook, Numerical solution of singular integral equations. In *Mechanics of Fracture*, (Edited by G. C. Sih), pp. 368–425. Noordhoff, Leyden, Netherlands (1973).
12. K. K. Lo, Analysis of branched cracks. *J. Appl. Mech.* **45**, 797–802 (1978).

APPENDIX A

The numerical solution of eqn (3.4) follows the method used by Lo[12]. A choice of time t is made. Applying the Gaussian integration formula, eqn (25.4.39) in [8], eqn (3.4) can be approximated by

$$\pi/n \sum_{i=1}^n \frac{f(v_i, (z/t)_k)}{v_i - (z/t)_k} F(v_i) + \pi/n \sum_{i=1}^n k(v_i, (z/t)_k) F(v_i) = H(z_k, t = \text{const.}),$$

$$k = 1, \dots, (n-1), \quad i = 1, \dots, n, \quad (\text{A.1})$$

where

$$v_i = V_{CT}(1 + \alpha_i)/2, \quad (\text{A.2})$$

$$\alpha_i = \cos[\pi(2i-1)/(2n)], \quad (\text{A.3})$$

$$(z/t)_k = V_{CT}(1 + \beta_k)/2, \quad (\text{A.4})$$

$$\beta_k = \cos(\pi k/n), \quad (\text{A.5})$$

$$H = t(z/t)g(z, t), \quad (\text{A.6})$$

and

$$z_k = (z/t)_k t, \quad (\text{A.7})$$

where t is considered to be a parameter. From the discussion in Section 3 on the behaviour of $\mu(v)$ as $v \rightarrow 0^+$, the condition $F(0) = 0$ must be imposed. This is approximated by requiring $F(v_n) = 0$. The result is a set of $(n-1)$ equations for $(n-1)$ unknowns $F(v_i)$, which can be easily solved. After a convergence study, $(n-1) = 20$ was used.

APPENDIX B

Koiter[4] has obtained the result for a static edge crack of depth l in a half plane subject to a uniform remote stress $(\sigma_{xx})_\infty$ in which the result is given in terms of an integral which, after numerical evaluation, gives $K = 1.12(\sigma_{xx})_\infty(\pi l)^{1/2}$.

If the limit $V_{CT} \rightarrow 0$, $t \rightarrow \infty$ such that $V_{CT}t \rightarrow l$ is taken in the dynamic problem with loading case (4), the static result may be obtained as a check case.

Small values of V_{CT} were taken and the results obtained at time t such that $l = tV_{CT}$. The calculated K values were within 3% of the static values obtained by Koiter and show the correct dependence on crack length.

For values of V_{CT} less than approximately $0.05/b$, the evaluation of the fundamental solution was not accurate. The problem lies in the evaluation of the σ_{xx} stresses for Problem 2 near the surface of the half plane where the difference of two large numbers must be calculated. It can be shown that for Problem 2, $\sigma_{xx} \rightarrow 0$ as $z \rightarrow 0$. However, although the ratio of the difference and the magnitude of the numbers is small (10^{-10} , which is close to the accuracy limit of the computer used), the value of the difference does not go to zero numerically and this causes problems in evaluating σ_{xx} . For larger values of V_{CT} , evaluations of σ_{xx} do not have to be made so close to the surface and the problem is avoided.

The accuracy of the results in the limiting case are considered to be evidence that the numerical calculations and technique were correct.